Soft Color Fields in DIS at low x and low Q^2

A. Metz
CEA-Saclay, DAPNIA/SPhN, F-91191 Gif-sur-Yvette, France
E-mail: ametz@cea.fr

Two complementary approaches to DIS at low x and low Q^2 are presented. In the first case we apply a model containig two Pomeron trajectories. In the second case we determine the gluon density in the semiclassical treatment at next-to-leading order. Both approaches rely on the concept of soft color fields.

1 Introduction

Regge-theory turned out to be very sucessful in describing the rise of hadronic cross sections by means of a so-called soft Pomeron trajectory. The same picture works well also for real photoabsorption on the proton. However, in the case of DIS with an incoming virtual photon and virtualities $Q^2 \geq 1\,\mathrm{GeV}^2$, HERA data show a clear deviation from a soft Pomeron behaviour of the cross section. Therefore, Donnachie and Landshoff [1] recently proposed a two-component model containig a soft and a hard Pomeron trajectory, where the influence of both components varies with Q^2. In the first approach [2] discussed below we also exploit a model with two Pomerons relating the soft Pomeron to non-perturbative QCD by means of the Model of the Stochastic Vacuum (MSV) of Dosch and Simonov [3]. This model can be considered as approximation to QCD in the infrared regime and provides, together with an ansatz for the quark wave function of the proton, a specific description of the soft color field of the proton. Our hard Pomeron is related to perturbative QCD.

In the second approach [4] we focus on the concept of parton densities frequently used in the analysis of DIS. More precisely, we determine in the semiclassical approach [5,6] the gluon density at next-to-leading order (NLO), which can serve as input in the evolution equations. In the semiclassical treatment of DIS the interaction of the partonic fluctuation of the virtual photon with the soft color field, describing the target at low x, is treated in an eikonal approximation [7]. Our result is quite general. The gluon density is expressed in terms of a (non-perturbative) Wilson loop and can be evaluated in any model of the soft color field of the target. On the other side, the concept of parton densities in general can not be continued to the real photon point. In that sense our second approach is more limited than the Pomeron model.

2 Soft and Hard Pomeron in DIS

For the structure function F_2 a model based on two Pomerons reads [1]

$$F_2(x,Q^2) = f_s(Q^2)x^{-\lambda_s} + f_h(Q^2)x^{-\lambda_h}, \tag{1}$$

where the exponents λ_s and λ_h of the soft and the hard contribution respectively do not depend on Q^2. We use $\lambda_s = 0$, and λ_h is treated as a free parameter. Though we can not explain the Pomeron intercepts, the residue functions f_s and f_h are related to QCD.

We evaluate f_s in the MSV, which is a specific model of non-perturbative QCD derived from the assumption that the infrared behaviour of QCD can be approximated by a Gaussian stochastic process [3]. In terms of the Wilson area law the MSV predicts linear confinement. The correlator of the gluon field strength, which has been computed on the lattice [8], serves as central quantity of the MSV. The lattice simulation of the correlator shows a transition between non-perturbative and perturbative effects roughly at the correlation length $a \approx 0.3\,\mathrm{fm}$. In the following we will exploit the scale a to separate soft and hard contributions.
In the eikonal approximation the cross section $\sigma_{q\bar{q}}$ for scattering a color dipole off the proton is energy independent in the MSV [9]. With the wave function $\Psi_{L,T}(Q^2,z,r)$ describing the fluctuation of a longitudinal or transverse photon into a $q\bar{q}$ pair, the soft part of the photoabsorption cross section on the proton takes the form

$$\sigma_{L,T}^{soft}(Q^2) = 2\pi \int_0^1 dz \int_a^\infty dr\, r |\Psi_{L,T}(Q^2,z,r)|^2 \sigma_{q\bar{q}}^{MSV}(z,r)\,, \tag{2}$$

where z is the longitudinal momentum fraction of the quark and r the transverse size of the fluctuation. To ensure confinement we use an effective quark mass [10] interpolating between a constituent quark at low Q^2 and a current quark at high Q^2. In Eq. (2) we introduce the lower cutoff a in the r integration [11], since the interaction at small distances is given by the hard component. According to $F_2^{soft} = Q^2(\sigma_L^{soft} + \sigma_T^{soft})/4\pi^2\alpha_{QED}$, we can compute the soft contribution from (2). The only free parameter of F_2^{soft} is the constituent quark mass [2].

To model F_2^{hard} we consider as starting point the evolution of a power-behaved F_2 derived by López and Ynduráin [12]. To leading order perturbative QCD implies that the singlet structure function reads

$$F_2^{pert}(x,Q^2) = C_2\,\alpha_s(Q^2)^{-d_+(1+\lambda)}x^{-\lambda}\,, \tag{3}$$

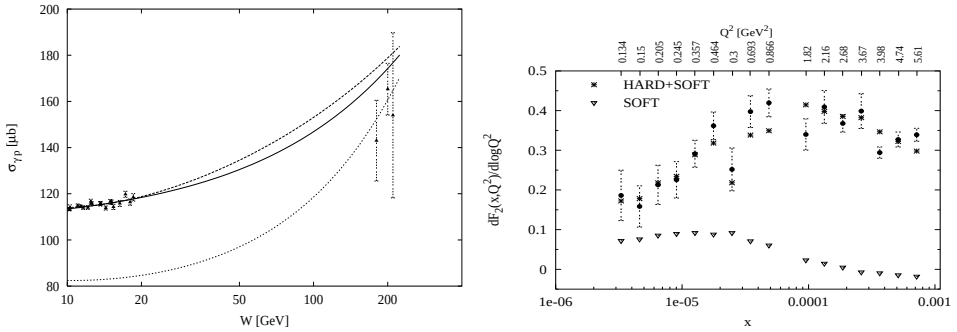

Figure 1:
Left panel: Total cross section for real photoproduction. Our fit (full line) is compared to those performed in Ref. [1] (dashed line) and in Ref. [13] (dotted line). Right panel: Logarithmic derivative of F_2 vs x.

with d_+ denoting the leading eigenvalue of the anomalous dimension matrix of the quark-singlet and gluon evolution kernel. The quantities C_2 and λ are free parameters. Eq. (3) is based on a singular gluon input and only valid at low x.
To obtain a hard component, which is suitable also at low values of Q^2, we multiply F_2^{pert} in (3) by a phenomenological factor and freeze the strong coupling. In doing so we introduce a further parameter (M), and have

$$F_2^{hard}(x,Q^2) = C_2\,\tilde{\alpha}_s(Q^2)^{-d_+(1+\lambda)}x^{-\lambda}\left(\frac{Q^2}{Q^2+M^2}\right)^{1+\lambda}, \qquad (4)$$
$$\text{with} \quad \tilde{\alpha}_s(Q^2) = \frac{4\pi}{\beta_0\,\ln((Q^2+M^2)/\Lambda^2_{QCD})}\,.$$

In particular, F_2^{hard} leads to a finite cross section $\sigma_{\gamma p}$ for real photoproduction. A different modification of F_2^{pert} in the region of low Q^2 has been proposed in Ref. [13]. Our complete ansatz for F_2 is given by the sum of F_2^{soft} and F_2^{hard}.

The four parameters of the model are fitted to data for real [14] and virtual [15] photoabsorption, where the kinematical cuts $Q^2 \leq 6.5\,\mathrm{GeV}^2$, $x \leq 0.01$ and $W \geq 10\,\mathrm{GeV}$ have been used to select the data. We obtain a $\chi^2/\mathrm{d.o.f} = 0.98$ for 222 data points and the exponent $\lambda_h = 0.37$.
On the l.h. side of Fig. 1 we have plotted our $\sigma_{\gamma p}$ in comparison with the fit of Donnachie and Landshoff [1], and Adel, Barreiro and Ynduráin [13]. The

parametrization of Ref. [13] has similarities to our approach but significantly underestimates the low energy data, which were not included in the fit. The r.h. side of Fig. 2 shows the logarithmic derivative of F_2 (Caldwell plot [16]). This picture demonstrates that in particular the turnover in the Caldwell plot can be described by a two-Pomeron model.
The extension of our model to higher values of Q^2 still has to be analysed. In addition, one has to investigate the consequences if the soft contribution is multiplied by the energy dependence of the soft Pomeron of hadron scattering.

3 The Semiclassical Gluon Distribution at Next-to-Leading Order

In the semiclassical approach, one considers, at low x, the proton as localized soft color field without specifying this field. DIS is treated in the target rest frame, where the photon acquires a partonic fluctuation. This picture of DIS allows for a combined description of both inclusive and diffractive events [17].

For extracting the gluon density it is convenient to use a 'scalar photon' (denoted by χ) coupled directly to the gluon field [18] via the lagrangian

$$\mathcal{L}_I = -\frac{\lambda}{2}\,\chi\,\mathrm{tr} F_{\mu\nu}F^{\mu\nu}\,. \tag{5}$$

The gluon density is derived by matching the semiclassical and the parton model approach. This means that to leading order we have to equate the cross section for the transition $\chi \to g$ in an external field with the cross section of the process $\chi g \to g$ as given in the parton model, where the former is evaluated in the eikonal approximation. To leading order one finds the result [6]

$$\begin{aligned} xg^{(0)}(x,\mu^2) &= \frac{1}{12\pi^2\alpha_s}\int d^2x_\perp \left|\frac{\partial}{\partial y_\perp} W^{\mathcal{A}}_{x_\perp}(y_\perp)\Big|_{y_\perp=0}\right|^2, \quad \text{where} \qquad (6)\\ W^{\mathcal{A}}_{x_\perp}(y_\perp) &= U^{\mathcal{A}}(x_\perp)U^{\mathcal{A}\dagger}(x_\perp+y_\perp)-1 \end{aligned}$$

is a Wilson loop in the adjoint representation, and the phase factor

$$U^{\mathcal{A}}(x_\perp) = P\exp\left[-\frac{ig}{2}\int_{-\infty}^{\infty} dx_+\, A^{\mathcal{A}}_-(x_+,x_\perp)\right] \tag{7}$$

governs the eikonalised interaction of a fast gluon in an external color field. The gluon distribution $xg^{(0)}(x,\mu^2)$ is a constant measuring the averaged local field strength of the target. Based on this leading order result, together with a logarithmic energy dependence introduced by hand, a sucessful description of DIS data has been obtained [6].

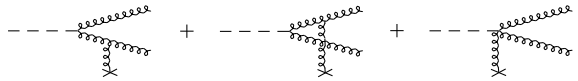

Figure 2:
Amplitude for $\chi \to gg$, which can be used to calculate the total semiclassical cross section in the high energy limit at NLO.

At NLO, we write the gluon density as

$$xg(x,\mu^2) = xg^{(0)}(x,\mu^2) + xg^{(1)}(x,\mu^2)\,, \tag{8}$$

with $xg^{(1)}(x,\mu^2)$ denoting the (scheme dependent) NLO correction. To extract this correction, the cross section for the transition $\chi \to gg$ in an external field has to be equated with the parton model cross section of the process $\chi g \to gg$. In the high energy limit, the total cross section $\chi \to gg$ [4] can be obtained from the eikonalized version of the diagrams in Fig. 2. Note that Fig. 2 just shows the leading contributions, which arise when expanding the eikonalized amplitude in powers of the external field. Because of the limited space, we quote here only the final result of the gluon density at NLO [4], given in the $\overline{\rm MS}$ scheme, without presenting any detail of the calculation:

$$xg^{(1)}(x,\mu^2) \;=\; \frac{1}{\pi^3}\left(\ln\frac{1}{x}\right)\int_{r(\mu)^2}^{\infty}\frac{dy_\perp^2}{y_\perp^4}\left\{-\int d^2x_\perp\,\mathrm{tr}\,W^{\mathcal{A}}_{x_\perp}(y_\perp)\right\}\,, \tag{9}$$

$$\text{with}\quad r(\mu)^2 = \frac{4e^{\frac{1}{12}-2\gamma_E}}{\mu^2}\,.$$

The scheme dependence of the gluon density enters through the short-distance cutoff $r(\mu)$. At NLO, the gluon density shows a $\ln(1/x)$ enhancement at small x, and is sensitive to the large-distance structure of the target.
If one exploits the model of a large hadron [19] to describe the color field of the proton, a comparison of our result with the one of Mueller [18,20] becomes possible. We find agreement for both the integrated distribution in (9) and the unintegrated gluon density [4] not shown here. However, in Refs. [18,20], where the main focus is on parton saturation, the scale dependence of the gluon density has not been discussed. More precisely, we provide for the first time a quantitative relation between the short-distance cutoff in Eq. (9) and the scale of the gluon distribution, which can only be achieved by matching the semiclassical approach with a treatment in the parton model.
The result (9) enables us to obtain numerical predictions for the gluon density at NLO in any non-perturbative approach describing the soft color field of the proton. In future work a comparison with DIS data has to be done using the semiclassical NLO distribution as input for the NLO evolution equations.

Acknowledgments

The results presented here emerged from an interesting and fruitful collaboration with U. D'Alesio, H.G. Dosch, A. Hebecker and H.J. Pirner. I am grateful to A. Hebecker for reading this manuscript. This work has been supported by the European TMR programme "Hadronic Physics with High Energy Electromagnetic Probes".

References

1. A. Donnachie and P.V. Landshoff, *Phys. Lett.* B **437**, 408 (1998).
2. U. D'Alesio, A.Metz and H.J. Pirner, *Eur. Phys. J.* C **9**, 601 (1999).
3. H.G. Dosch, *Phys. Lett.* B **190**, 177 (1987); H.G. Dosch and Yu.A. Simonov, *Phys. Lett.* B **205**, 339 (1988).
4. H.G. Dosch, A. Hebecker, A. Metz and H.J. Pirner, hep-ph/9909529.
5. W. Buchmüller, M.F. McDermott and A. Hebecker, *Nucl. Phys.* B **487**, 283 (1997); B **500**, 621 (1997) (E).
6. W. Buchmüller, T. Gehrmann and A. Hebecker, *Nucl. Phys.* B **537**, 477 (1999).
7. O. Nachtmann, *Ann. Phys.* **209**, 436 (1991).
8. A. Di Giacomo and H. Panagopoulos, *Phys. Lett.* B **285**, 133 (1992).
9. H.G. Dosch, E. Ferreira and A. Krämer, *Phys. Rev.* D **50**, 1992 (1994).
10. H.G. Dosch, T. Gousset and H.J. Pirner, *Phys. Rev.* D **57**, 1666 (1998).
11. See also: M. Rüter, *Eur. Phys. J.* C **7**, 233 (1999).
12. C. López and F.J. Ynduráin, *Nucl. Phys.* B **171**, 231 (1980).
13. K. Adel, F. Barreiro and F.J. Ynduráin, *Nucl. Phys.* B **495**, 221 (1997).
14. D.O. Caldwell et al., *Phys. Rev. Lett.* **40**, 1222 (1978); H1: S. Aid et al., *Z. Phys.* C **69**, 27 (1995); ZEUS: M. Derrick et al., *Phys. Lett.* B **293**, 465 (1992); Zeus: M. Derrick et al., *Z. Phys.* C **63**, 391 (1994).
15. H1: S. Aid et al., *Nucl. Phys.* B **470**, 3 (1996); H1: C. Adloff et al., *Nucl. Phys.* B **497**, 3 (1997); ZEUS: M. Derrick et al., *Z. Phys.* C **69**, 607 (1996); ZEUS: M. Derrick et al., *Z. Phys.* C **72**, 399 (1996); ZEUS: J. Breitweg et al., *Phys. Lett.* B **407**, 432 (1997); NMC: M. Arneodo et al., *Nucl. Phys.* B **483**, 3 (1997); E665: M.R. Adams et al., *Phys. Rev.* D **54**, 3006 (1996).
16. A. Caldwell, DESY Theory Workshop (1997).
17. For an extensive review on the semiclassical approach and diffraction in DIS see: A. Hebecker, hep-ph/9905226.
18. A.H. Mueller, *Nucl. Phys.* B **335**, 115 (1990).
19. L. McLerran and R. Venugopalan, *Phys. Rev.* D **49**, 2233 (1994).
20. A.H. Mueller, hep-ph/9904404.